Heat Transfer Origin of Thermal Shock Fracture and its Application for LWR Fuel during Reflood

Youho Lee and Hee Cheon NO
Korea Advanced Institute of Science and Technology (KAIST)
291 Daehak-ro, Yuseong-gu, Daejeon 305-338
euo@kaist.ac.kr; hcno@kaist.ac.kr

ABSTRACT

In water quenching, a solid experiences dynamic heat transfer rate evolutions with phase changes of the fluid over a short quenching period. Yet, such a dynamic change of heat transfer rates has been overlooked in the analysis of thermal shock fracture. In this study, we are presenting quantitative evidence against the prevailing use of a constant heat transfer coefficient for thermal shock fracture analysis in water. We conclude that no single constant heat transfer could suffice to depict the actual stress evolution subject to dynamic heat transfer coefficient changes with fluid phase changes. Use of the surface temperature dependent heat transfer coefficient will remarkably increase predictability of thermal shock fracture of brittle materials and complete the picture of stress evolution in a quenched solid. The presented results show stress prediction around ~90% of the actual fracture stress with the use of the surface temperature dependent heat transfer coefficient, implying that fracture uncertainties predominantly remain in the statistical nature of brittle fracture. For thermal shock fracture analysis of fuel rods during LWR reflood, transient sub channel heat transfer coefficients obtained from a thermal-hydraulics code should be used as input to stress analysis. Such efforts will advance of thermal shock modeling, which will introduce a fundamental improvement over the currently practiced experimental empiricism for cladding fracture analysis during reflood. This study advocates that advanced boiling study on fuel rod surface should consider effects of surface oxide scale, crud, and surface pore structures which naturally arise in the course of the reactor operation.

1. INTRODUCTION

Thermal shock fracture is an important phenomenon that often sets the maximum service temperature of a brittle material. This is also true for nuclear reactors. In a light water reactor (LWR), mechanical behavior of fuel rods upon thermal shock during reflood quenching is a key to the reactor safety. That, retention of oxidized cladding ductility after reflood quenching sets the maximum allowable temperature (~1204ºC) in loss of coolant accidents (LOCA). This temperature limit is prescribed in the current emergency core cooling system criteria of U.S Nuclear Regulatory Commission (U.S. NRC), 10 CFR 50.46. It is noteworthy that the quantification of thermal shock damage for embrittled zircaloy in 10 CFR 50.46 is based on highly empirical experimental investigations, which lack a fundamental analysis of thermal stresses. Such an empirical treatment of thermal shock damage in the regulation results in limiting its assurance even under small departures from the reference experimental conditions. As a consequence, technical skepticism on the current 10 CFR 50.46 for today's fuel rods of unprecedentedly aggressive operations is being raised,

triggering an organized movement for revisiting it. Thermal shock fracture is also important for advanced cladding materials. Today, fully ceramic materials such as silicon carbide, or surface modified zircaloy with oxidation suppression coatings are considered as potential alternative to zircaloy. For those emerging claddings, brittle thermal shock fracture is still an important failure mechanism. For ductile cladding materials, formation of brittle phases with irradiation-damage, oxygen and hydrogen influence, and surface oxide scale makes brittle-fracture a relevant failure mechanism upon thermal shock. For ceramic claddings, the entire cladding thickness is essentially brittle without appreciable plasticity, undergoing brittle fracture upon thermal shock. Yet, our understanding of brittle fracture remains in the realm of experimental empiricism without a fundamental analytic capability. Such a lack of profound understanding of thermal shock fracture significantly challenges the assurance of integrity of the current zircaloy cladding in increasingly aggressive operating conditions with extended accident scenarios as well as advanced cladding developments.

Understanding thermal shock fracture of a brittle material requires (1) heat transfer rate between the solid and the fluid for transient temperature fields of the solid, and (2) structural response of the solid under the obtained transient temperature fields. In water quenching, a solid experiences dynamic time-varying heat transfer rates with phase changes of the fluid over a short quenching period [1]. Yet, such a dynamic change of heat transfer rates during the water quenching transience has been overlooked in assessments of mechanisms, predictability, and uncertainties for thermal shock fracture [2-12]. Rather, a time-constant heat transfer coefficient, named 'effective heat transfer coefficient' has become a conventional input to thermal shock fracture analysis [2,4-6,10,11,13-17]. Our understanding of heat transfer origin of thermal shock fracture has been loosely rationalized, based on the order of magnitudes of effective heat transfer coefficients. It has been generally believed that the effective heat transfer coefficient in the range of $10^4 \sim 10^5$ W/m^{2}K is required for a series of observed thermal shock fractures for Al_2O_3 [5,6,10,17,18]. Such prevailing use of a constant heat transfer coefficient has inevitably led to an incomplete picture of the stresses in the ceramic. Yet, it is remarkable to note how small attention and efforts have been given to resolve effects of heat transfer coefficient inputs in thermal shock fracture studies. Among other variable parameters, heat transfer coefficient introduces the largest uncertainties in stress evaluation in the ceramic. Hence, it is timely, if not too late, to conduct a dedicated study to establish a fundamental modeling capability on thermal-hydraulic and mechanical coupling for an advanced thermal shock analysis. In this study, we (1) explore effects of heat transfer coefficient on thermal shock fracture analysis and prediction in water quenching, (2) assess the current prevailing use of constant heat transfer coefficient, and (3) propose an advanced heat transfer coefficient treatment, and (4) discuss its applications LWR fuels.

2. CONVENTIONAL TREATMENTS OF CONSTANT HEAT TRANSFER COEFFICIENTS

For a slab, the effective heat transfer coefficient h_{eff} can be obtained by finding the condition when the maximum surface stress in cold shock meets the fracture stress σ_f at the slab surface ($\pm L$) using the following relation [11]

$$\sigma_f(\pm L, t^*) = \frac{\bar{E}\bar{\alpha}(T_i - T_\infty)}{\left\{1.5 + \frac{3.25}{Bi} - 0.5e^{-16/Bi}\right\}} \tag{1}$$

where $\bar{E} = \frac{E}{1-\nu^2}$, $\bar{\alpha} = \alpha + \nu\alpha$, E is Young's modulus, ν is Poisson's ratio, T_i is the initial temperature of the material, T_∞ is the water bath temperature, and Bi is the Biot number, defined as $h_{eff}L/k$, L is the half of the specimen thickness, and k is the thermal conductivity of the material. The time for the surface to reach the fracture stress t^* is

$$t^* = \frac{0.48}{1 + 1.8Bi}\left(\frac{L^2}{\alpha_{diff}}\right) \qquad (2)$$

where α_{diff} is the thermal diffusivity of the material.

Fig. 1 summarizes the effective heat transfer coefficients (Eq.(1)) and time for fracture (Eq.(2)), for various past experiments (with most them from Al_2O_3 and Si_3N_4) that report essential inputs to Eqs.(1) and (2).
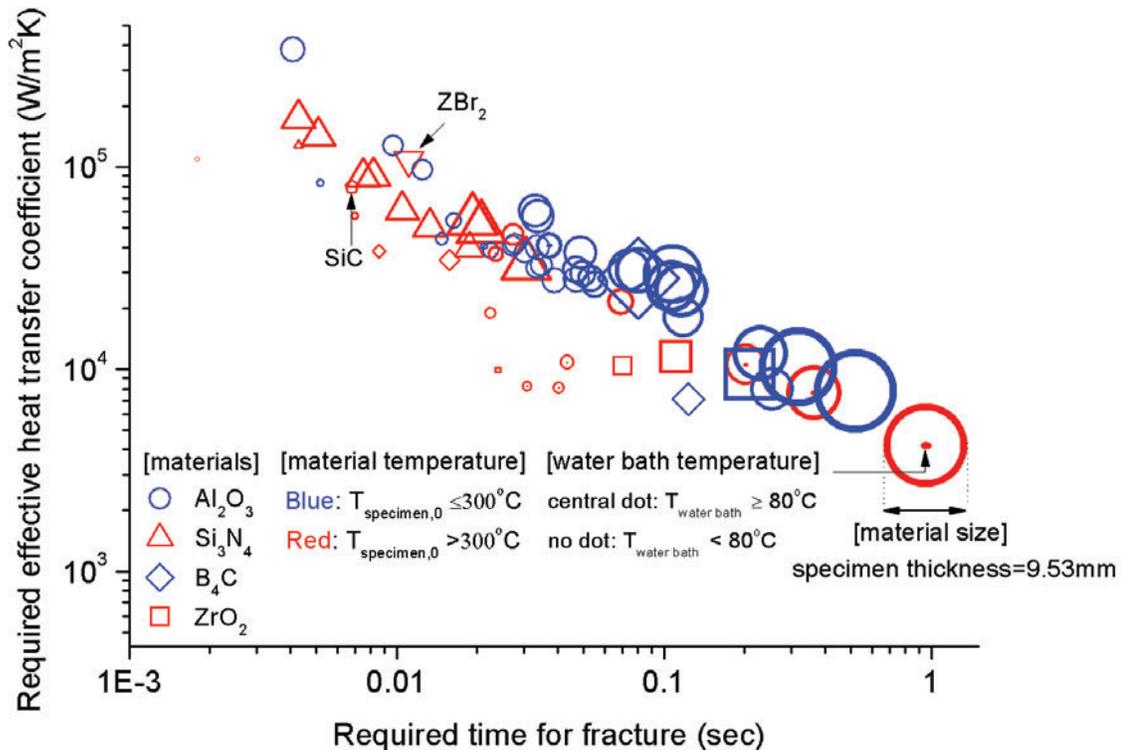

Figure 1. Required effective heat transfer coefficients and time for fracture obtained with Eq.(1) and (2), respectively, from various past thermal shock experimental data that provide fracture stress, critical temperature difference, water bath temperature, and specimen size. Presented specimens are selected from past studies [2,4-6,9,10,13,14,19,20-22]

A few obvious trends can be inferred from Fig. 1. Firstly, smaller specimens require higher effective heat transfer coefficients for fracture to occur. In addition, Si_3N_4 generally requires higher effective heat transfer coefficients than Al_2O_3 with a higher specimen quenching temperature. Those observations are closely attributed to material-sensitive nucleate and transition boiling characteristics. Such high heat transfer coefficients well above ~10^4 W/m²K are generally considered to be not attainable with presence of a thick vapor blanket in film boiling, but it is a result of repetition of local bubble formation, detachment, and subsequent water quenching on the surface during nucleate and transition boiling modes. The heat transfer rate upon the local instant water quenching after the bubble departure during a bubbly heat transfer mode is modeled by an instant solid-liquid conduction of the semi-infinite media [23,24], whose surface heat flux

rate is given as $q'' = \pm \frac{k(T_{int} - T_i)}{(\pi \alpha t)^{1/2}}$ with T_{int} being the interface temperature upon contact. Theoretically, the heat flux is infinity at t=0 but such a singularity in heat transfer rates do not contribute to fracturing the material because it remains in infinitesimal (x→0) distance from the surface. While the local solid-liquid contact is the origin of high heat transfer rates during the bubbly heat transfer modes, many thermo-physical parameters determine the degree of it by controlling contact frequency, bubble site density, and the interface temperature. It has been well-understood in two-phase heat transfer community that smaller specimen size, and higher wettability of a solid surface promote the solid-liquid contact heat transfer [1], resulting occurrence of solid-liquid contact at an elevated temperature. Our knowledge on the wettability of Si_3N_4 and Al_2O_3 agrees with the observed trend: Si_2N_4 (~ 30°) has better wettability than Al_2O_3 (~80°), with the smaller contact angle [25-27]. Indeed, some engineered low wettability surfaces were proven to significantly reduce the danger of thermal shock fracture [28,29] by obliterating the bubbly heat transfer modes with enhanced vapor insulation throughout the cooling transience. Liang et. al [30] conjecture a lower effective heat transfer coefficient for the oxidized surface of ZrB_2-SiC-AlN ceramic composite than the bare surface of the material after finding the elevated critical temperatures of the oxidized specimens. This explanation may also be reflected in the change of surface wettability with oxide formation. The presented constant heat transfer coefficients in Fig.1 are coherent with the observed thermal shock fractures. Yet, they may not satisfy the actual heat transfer rate from the heat transfer point of view as they were obtained as to solely satisfy observed fractures.

3. STRESS EVOLUTION WITH SURFACE TEMPERATURE DEPENDENT HEAT TRANSFER COEFFICIENT, $h(T_s)$

Although effective heat transfer coefficients, based on the structure point of view, provide us ideas for (1) heat transfer characteristics of different surfaces, and (2) fracture-inducing heat transfer modes based on the order of magnitudes (i.e: bubbly heat transfer or vapor film heat transfer), they have a limited physical significance as they do not take into account the actual time-varying heat transfer coefficients. That is, although effective heat transfer coefficients satisfy observed thermal shock fractures from the structural mechanics point of view, they are not coherent with the actual heat transfer physics from the thermal-hydraulic point of view. Such loose establishments between the mechanical and the thermal-hydraulic treatments of heat transfer coefficients have resulted in poor rationalization for the choice of heat transfer coefficients for thermal shock fracture prediction and analysis. In this study, we investigate heat transfer origin of thermal shock fracture in water quenching by exploring an establishment for a heat transfer rate treatment coherent for both structure and thermal-hydraulics.

A very limited amount of experimental resource is available for heat transfer rate of brittle materials due to difficulties in installing thermos-couples in the body of ceramics, and relatively less emphasized engineering importance. The measurement of a temperature dependent heat transfer coefficient of Al_2O_3 rod with diameter 50mm in water quenching by Zhou et. al.,[31] shown in Fig. 2(b) is a very useful resource. Surface heat flux in Fig. 2a is obtained with the relation, $q'' = h(T_s)(T_s - T_\infty)$. In this study, a high speed video camera was used to record boiling transience of Al_2O_3 with thickness of 6.35mm, Fig. 2(c).
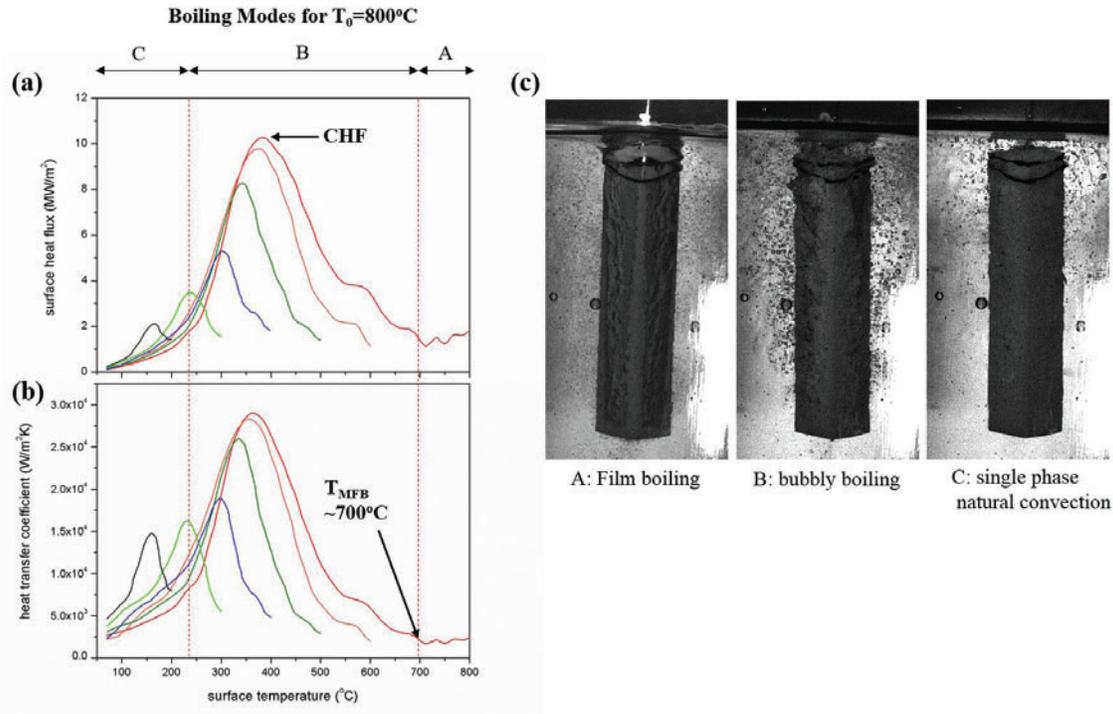
Figure 2. (a) surface heat flux of Al_2O_3 specimen calculated using heat transfer coefficient data of Zhou et. al., [31] shown in Fig.2b. (b) experimentally obtained heat transfer coefficients for Al_2O_3 quenched in water bath $T_\infty=20°C$ for different initial specimen temperatures $T_0=200, 300, 400, 500, 600,$ and $800°C$ by Zhou et al., [31]. (c) different boiling modes for the indicated boiling regimes (A, B, and C in Fig. 2(a)and (b)) with Al_2O_3 specimen of thickness 6.35mm

When the surface temperature is above the minimum film boiling temperature (T_{MFB}), stable film is established (See Fig. 2(c)), characterized with low heat transfer coefficients. As the solid surface cools below T_{MFB}, heat transfer is enhanced as the stable vapor film breaks, undergoing a mixed boiling mode consisting of nucleation and intermittent vapor film insulation. This stage of boiling is referred as the transition boiling mode. The heat transfer rate continues to increase until the surface reaches critical heat flux (CHF), with the overriding effect of diminishing contribution of intermittent vapor insulation. At the CHF point, the surface experiences the highest heat transfer rate over the entire quenching transience. Upon the further cooling of the surface below the CHF point, the surface heat transfer predominantly occurs through local nucleation of vapor (nucleate boiling mode) until it reaches temperature that does not cause a vapor formation (single phase natural convection). The surface heat transfer rate rapidly changes during the transition, CHF, and nucleate boiling mode; all of them commonly involve vapor bubble formation in the heat transfer mechanism. Hence, those three groups are referred as the 'bubbly' boiling mode (mode B in Fig. 2). It is shown in Fig. 2 that when materials are quenched below T_{MFB}, hystereses in surface heat flux and heat transfer coefficients are evident.

In this study, we investigate stress evolution of quenched specimen with the actual heat transfer coefficients as a function of surface temperature $h(T_s)$ shown in Fig. 2(b). Instead of using a constant heat transfer coefficient, the heat transfer coefficients are treated as a function of temperature, $h(T)$ to yield the following set of energy equation and boundary condition for a slab of thickness 2L

$$\frac{1}{\alpha}\frac{\partial T}{\partial t} = \frac{\partial^2 T}{\partial x^2} \quad \text{with B.C} -k\frac{\partial T}{\partial x}\Big|_{x=\pm L} = h(T_s)(T(x = \pm L, t) - T_\infty) \tag{3}$$

With the obtained temperature fields T(x,t), the stress distribution in the slab was calculated with the following relation [11],

$$\sigma(x,t) = -\bar{E}\bar{\alpha}(T - T_i) + \frac{\bar{E}\bar{\alpha}}{2L}\int_{-L}^{L}(T - T_i)dx \tag{4}$$

Fig. 3 shows that the surface temperature dependent heat transfer coefficient $h(T_s)$ gives a remarkably different result for surface temperature and stress evolution compared to the constant average heat transfer coefficient $(h(T_s)_{avg}=1.05 \times 10^4$ W/m-K for $T_0=800$ ^oC [31]) during a quenching transience. Use of the average heat transfer coefficient yields marked errors in predicting both the peak surface stress and the time for it as well as the surface temperature. This demonstrates that use of the average heat transfer coefficient $h(T_s)_{avg}$ does not necessarily guarantee to yield the actual stress evolution. Note that Zhou et al., [31] found that $h(T_s)_{avg}$ values of temperature dependent $h(T_s)$ fall within the range of previously proposed effective heat transfer coefficients $10^4 \sim 10^5$ W/m^{2}K for Al_2O_3, and justified the use of $h(T_s)_{avg}$ as a constant heat transfer coefficient input to thermal shock fracture analysis. The presented results in Fig.3 that the conclusion of Zhou et al., [31] is misleading. The average heat transfer coefficient $h(T_s)_{avg}$ may simplify a calculation in terms of matching an amount of energy transfer integrated over a time period, but it has no explicit physical significance in terms of yielding a temperature gradient relevant to thermal shock fracture. The difference in surface stress evolution between $h(T_s)$ and $h(T_s)_{avg}$ is pronounced for a case that involves rapidly varying heat transfer modes with time. In case of Fig. 3a, the specimen is quenched from 800^oC, experiencing film, bubbly, and natural convection in sequence. For a quenching transience that involves the initial film boiling heat transfer mode shown in Fig. 3, the average heat transfer coefficient $h(T)_{avg}$ significantly overestimates the early stress increase rate, predicting an earlier fracture of the material. This is attributed to neglecting the film boiling period during which the material experiences a relatively slowly growing stress with time. In Fig. 3, the structural integrity of the quenched specimen is most severely challenged during the bubbly boiling mode after the end of the film boiling period. Nevertheless, one should be cautious in saying the time at which a quenched specimen is fractured. It is inferable from Fig. 3a that for a thicker Al_2O_3 specimen ($\delta > 5$mm) when quenched from 800^oC, even the film boiling mode may cause thermal shock fracture by bringing the surface stress greater than ~200MPa. Likewise, a very thin Al_2O_3 ($\delta \ll 5$mm) is anticipated almost certainly to fracture during the bubbly heat transfer mode when quenched from 800^oC.
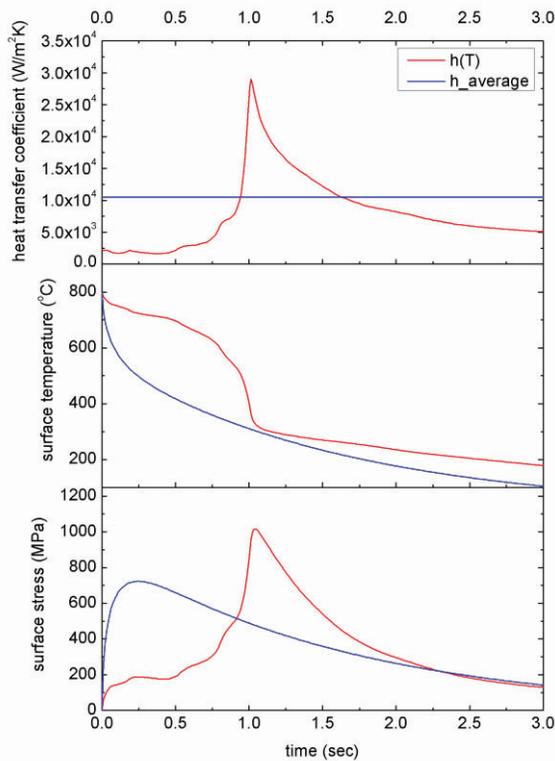
Figure 3. (a) comparisons of heat transfer coefficient, surface temperature (calculated), and surface stress (calculated) with surface temperature dependent heat transfer coefficient $h(T_s)$ [31] and with the average heat transfer coefficient $h(T_s)_{avg}$ for 5mm thick Al_2O_3 of 800°C quenched into 20°C water bath.

From a practical point of view, the prime importance of discussing heat transfer origin of thermal shock fracture is centered upon predictability of thermal shock fracture. Indeed, general consensus has been made in the thermal shock community that uncertainties on heat transfer coefficient have become a major limit for thermal shock fracture predictability in water. An effective heat transfer coefficient h_{eff} is obtainable only with material fracture data after quenching; it is more appropriately used as a post-fracture analysis parameter than that of a fracture-prediction. Fig. 4 shows calculated time-dependent surface stress changes for Al_2O_3 specimens quenched from critical temperatures around ~ 200°C in water bath around ~20°C with inputs of $h(T_s)$, $h(T_s)_{avg}$, and h_{eff}. Note h_{eff} is calculated from thermal shock fracture data with Eq.(1). Hence, in Fig. 4, the effective heat transfer coefficients, h_{eff} give peak surface stresses equal to the fracture stress σ_f at time t^*. The temperature dependent heat transfer coefficient $h(T_s)$ markedly underestimates the peak surface stresses in Fig. 4. This is primarily attributed to the mismatch in the specimen sizes of the presented ones (4, 6, and 12mm [4,10,13]) with $h(T_s)$ measurement ~50mm [31]. Note that $h(T_s)$ measured by Zhou et. al., [31] are limited to the specimen size ~50mm, which is larger than most of the water quenched specimens of past studies. Larger specimen sizes are known to decrease bubbly boiling heat transfer coefficients with a lower CHF point and T_{MFB}, primarily through the increased difficulty of bubble escape, with a presence of the maximum size beyond which no appreciable decrease in heat transfer rate is observed [1,32,33]. Hence, the heat transfer coefficients $h(T_s)$ in Fig. 2 should be regarded as underestimated values for quenched Al_2O_3 specimens presented in most of studies. In that regard, it is remarkable to note increasing predictability of fracture stress with $h(T_s)$ as the specimen size increases towards that of $h(T_s)$

measurement (50mm) in Fig. 4. Al_2O_3 quenched from the critical temperature around ~ 200°C in ~20°C water bath undergoes a relatively short bubbly boiling period without an initial film boiling mode (Fig. 2). This may explain the apparent coincidence in the time t^* for the peak surface stresses of $h(T_s)$ with ones calculated with $h(T_s)_{avg}$ and h_{eff}, as shown in Fig. 4.
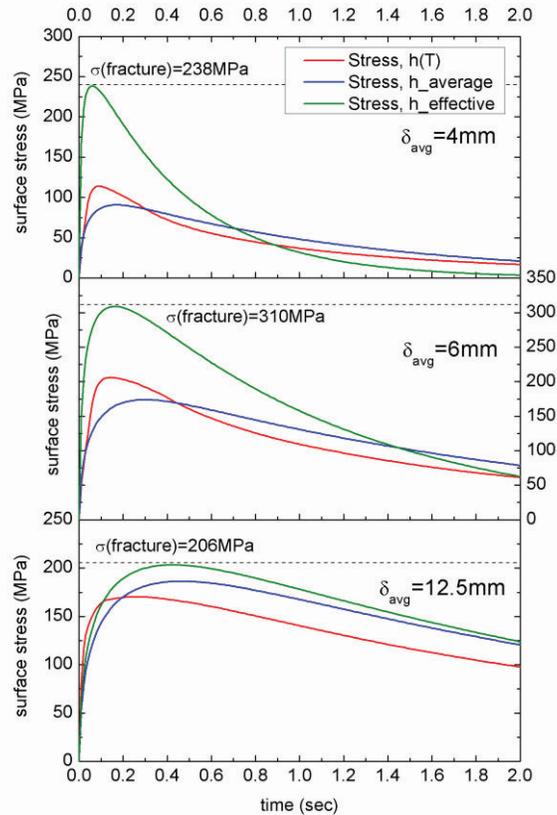

Figure 4. Surface stress evolution with different inputs of heat transfer coefficients ($h(T_s)$ [31], $h(T_s)_{avg}$, and h_{eff}) for increasing material thicknesses of Al_2O_3 quenched from the critical temperatures for thermal shock fracture. h_{eff} were calculated from Eq.(1) with inputs from experiments (Al_2O_3 experimental data: 4mm [5], 6mm [10], and 12.5mm [13]).

4. THERMAL SHOCK FRACTURE PREDICTABILITY WITH $h(T_s)$: PHYSICALLY COHERENT INPUT TO THERMAL SHOCK FRACTURE ANALYSIS

Unfortunately, no experimental data for $h(T_s)$, to our knowledge, has been obtained for Al_2O_3 specimen sizes that match the past thermal shock data presented in this study. Hence, at this stage, our best rationale about predictability of thermal shock fracture with the input of $h(T_s)$ would be to see its improvement with increasing convergence of quenched Al_2O_3 size with that of $h(T_s)$ measurements. Fig. 5 summarizes predictability of various Al_2O_3 specimens with respect to their size normalized to that of the $h(T_s)$ measurement. A strong positive relation holds between the normalized specimen thickness and the

normalized stress. This demonstrates that the apparent errors in predicting thermal shock fracture with $h(T_s)$ in Fig. 4 are due to the mismatch of the specimen size between the quenched and the $h(T_s)$ measured. Hence, accurate input of temperature-dependent heat transfer coefficient $h(T_s)$ specific to the quenched specimen would be necessary to accurately predict thermal shock fracture. The presented predictability above ~80% of the true fracture stresses is remarkable considering the inherent uncertainties of thermal shock fracture analysis. It means that once the surface temperature-dependent heat transfer coefficient $h(T_s)$ is measured/or known, the uncertainties in prediction of thermal shock fracture will only remain the statistical nature of brittle fracture, resulting in an enhanced predictability of it to the level of general load induced fracture.
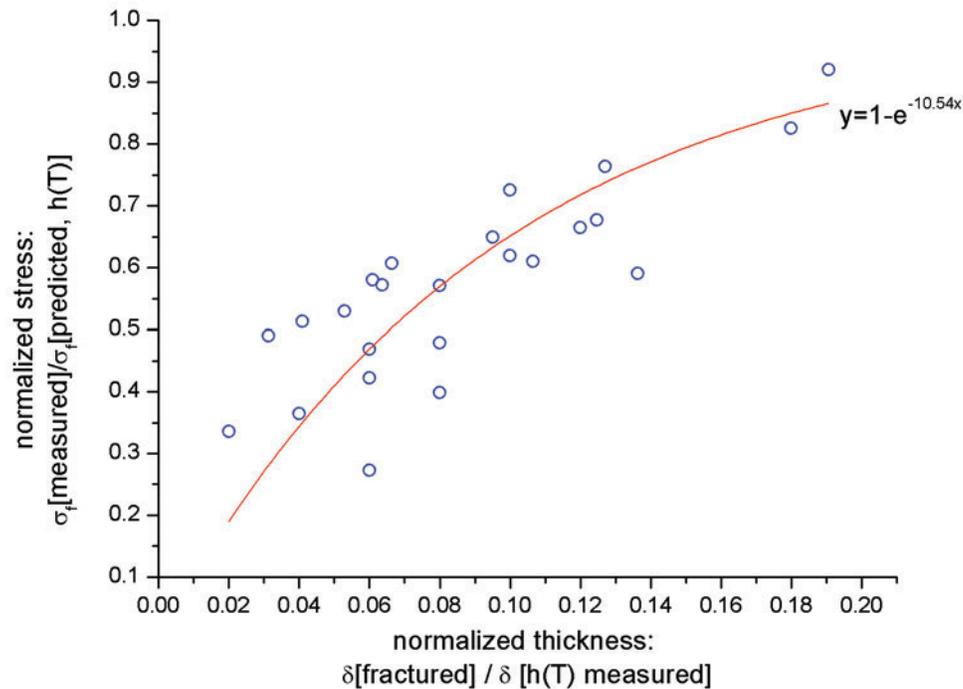

Figure 5. predictability of fracture stress with temperature dependent heat transfer coefficient $h(T_s)$ with the diminishing difference between the quenched specimen thickness δ[fractured] [2,5,6,10,13,20,22] and the specimen thickness where $h(T_s)$ measured δ[fractured][31] (the positive relation accounts for increasing thermal shock fracture predictability with an accurate input of $h(T_s)$. Al_2O_3 specimens quenched in the identical water bath temperature ($20 \pm 5°C$) of the $h(T_s)$ measurement were selected)

The presented predictability of thermal shock fracture in Fig.5 delivers a few important messages to the thermal shock fracture community. That, input of the actual surface temperature dependent heat transfer coefficient is a key to accurately predict stress evolution in the solid. No single constant heat transfer coefficient suffices to simulate the actual stress evolution. Yet, such an axiomatic argument is not being practiced in thermal shock communities – today, use of the surface temperature dependent heat transfer coefficient is residing in the realm of unpracticed generality. Study of boiling has been a traditional realm of mechanical engineers. Most of our understanding on transient boiling in quenching is limited to metal-based surfaces with highlights on its application for nuclear fuel cooling in accidents in boiling water.

Efforts on measurements of boiling heat transfer coefficients of brittle materials quenched in water have been extremely limited because of limited understanding of its engineering importance in the past.

5. APPLICATION TO LWR REFLOOD in LOCA

LWR core during reflood is an extreme example of dynamic heat transfer modes with complex phase change phenomena. Modeling such dynamic two-phase phenomena has long been a key task for thermal-hydraulics. With the extensively accumulated experimental data and modeling experience, RELAP-5 3D is now the state of the art computer code for transient simulation of LWR coolant systems during postulated accidents used by U.S NRC. As a beginning step to investigate the effect of dynamic heat transfer evolution, a reflood phase during LBLOCA in 3479 MWth PWR was simulated with RELAP-5 3D. Fig.6 shows the RELAP-5 3D nodalization scheme (Fig.6a), the cladding surface temperature (Fig.6b), and the heat transfer coefficients (Fig.6c).
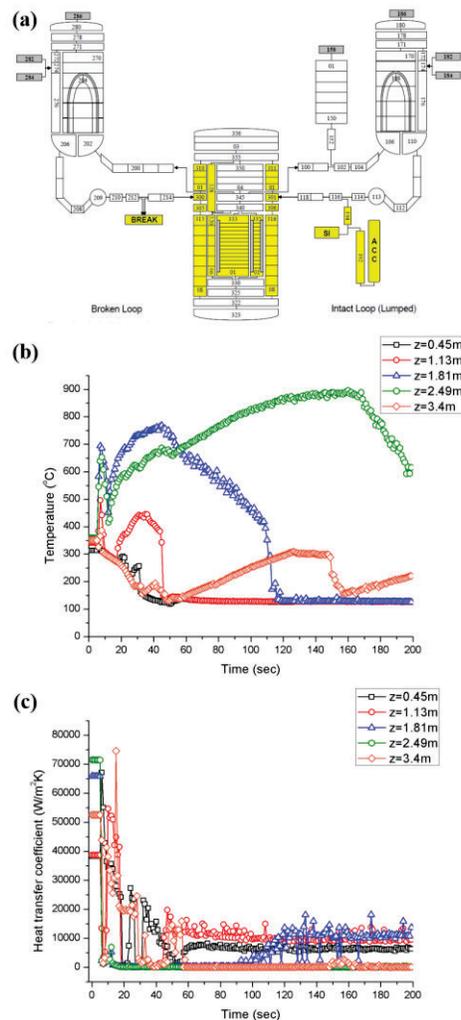

Figure 6. RELAP-5 3D results for the reference LBLOCA: (a) RELAP-5 3D LBLOCA nodalization scheme [Figure in courtesy of R. Hu [34]] (b) cladding outer surface temperature and (c) local heat transfer coefficients with respect to axial location z

It is clearly shown in Fig.6c that the cladding experiences dynamic, even chaotic, heat transfer mode evolutions overarching from film boiling to violent nucleate boiling. With convective effects, the presented sub-channel dynamic heat transfer evolution is far more pronounced than the discussed reference in Fig.3~5. It is inferable in Fig.6 that no single constant heat transfer would be possible to replace the presented ranges of dynamic heat transfer coefficients in a sub-channel.

Therefore, for cladding thermal fracture analysis, time-dependent heat transfer coefficients of subchannel should be used for cladding stress analysis; use of the realistic transient heat transfer coefficient should be practiced in order to depict the actual stress evolution. This calls for a need for a platform that couples a thermal-hydraulics code with a structural analysis model. A more fundamental issue is on the material-specific heat transfer coefficient models. The current thermal hydraulic analysis code, e.g., RELAP-5 3D, uses heat transfer coefficients found for zircaloy surface. Boiling characteristics are submissive to significant changes with numbers of surface character-specific parameters including surface wettability, pore structure, and roughness, etc. This is an issue for improving thermal-hydraulic modelling accuracy. From the thermal shock fracture point of view, surface character-specific heat transfer models are also of critical importance. A few past investigations report a marked difference between the fracture initiating temperature between the bare specimen and surface modified specimens [28,30]. Particularly, formation of oxide layer on the surface [30] changes thermal shock fracture behavior. This illuminates that an advanced boiling study on fuel rod surface should consider effects of surface oxide scale (ZrO_2), crud, and surface pore structures which naturally arise in the course of the reactor operation.

6. Conclusions

In this study, we are presenting quantitative evidence against the prevailing use of a constant heat transfer coefficient for thermal shock fracture analysis in water. No single constant heat transfer could suffice to depict the actual stress evolution subject to dynamic heat transfer coefficient changes with fluid phase changes. Use of the surface temperature dependent heat transfer coefficient will remarkably increase predictability of thermal shock fracture of brittle materials and complete the picture of stress evolution in the quenched solid. The presented result with Al_2O_3 shows stress prediction around ~90% of the actual fracture stress with the use of the actual surface temperature dependent heat transfer coefficient. Hence, this work formerly informs thermal shock community that the surface temperature dependent heat transfer coefficient $h(T_s)$ should be used for thermal shock fracture analysis and prediction. Yet, it is remarkable to note how widely, without technical consciousness, the use of a constant heat transfer coefficient has been practiced in the field of thermal shock fracture studies. A surface temperature dependent heat transfer coefficient $h(T_s)$ is dependent on a number of parameters, including water bath temperature, pressure, specimen size and shape, and surface characteristics including wettability, nucleation site density, and pore structures. Hence, for a thermal shock fracture analysis, those non-strength related thermal shock fracture parameters should be accounted in $h(T_s)$. Consequently, increasing efforts should be made on understanding transient boiling heat transfer rates of brittle materials to advance our understanding of thermal shock fracture. For LWR applications, a structural platform that uses transient sub channel heat transfer coefficients obtained from a thermal-hydraulics code is needed. Advanced boiling study on fuel rod surface should consider effects of surface oxide scale (ZrO_2), crud, and surface pore structures which naturally arise in the course of the reactor operation.

ACKNOWLEDGMENTS

REFERENCES

1. S.G. Kandlikar, M. Shoji, V.K. Dhir, Handbook of Phase Change: Boiling and Condensation, Taylor & Francis, Philadelphia, 1999.
2. J. Absi, J.C. Glandus, J. European Ceramic Society. **24** (2004) 2835-3838.
3. W. Zhi, Q. Qiang, W. Zhanjun, S. Guodong, Materials and Design. **32** (2011) 3499-3503.
4. J. She, J. Yang, D.D. Jayaseelan, N. Kondo, T. Ohji, S. Kanzaki, J. Am. Ceram. Soc. **86** [4] (2003) 738-40.
5. J.C. Glandus, P. Boch, Int. J. Thermophysics. **2** (1981) 89-101.
6. J.P. Singh, Y. Tree, D.P.H. Hasselman, Journal of Materials Science. **16** (1981) 2109-2118.
7. H. Wang, R.N. Singh, International Materials Reviews. **39** (1994) 228-244.
8. T. Nishikawa, T. Gao, M. Hibi, M. Takasu, Journal of Materials Science. **29** (1994) 213-217.
9. J.W. Zimmermann, G.E. Hilmas, W.G. Fahrenholtz, Materials Chemistry and Phsyics. **112** (2008) 140-145.
10. D. Sherman, D. Schlumm, Scripta Mater. **42** (2000) 819-825.
11. T.J. Lu, N.A. Fleck, Acta Mater. **46** (1998) 4755-4768.
12. G.A. Schneider, Ceramics International. **17** (1991) 325-333.
13. M. Fellner, P. Supancic. Key Engineering Materials. **223** (2002) 97-106.
14. M.Ishitsuka, T. Sato, T. endo, M. shimada, Journal of Materials Science Letters. **24** (1989) 4057-4061.
15. J. Liang, C. Wang, Y. Wang, L. Jiang, and X. Luan, Scripta Mater. **61** (2009) 656-659.
16. M. Collin, D. Rowcliffe, Acta Mater. **48** (2000) 1655-1665.
17. C.P. Jiang, X.F. Wu, J. Li, F. Song, Y.F. Shao, X.H. Xu, P. Yan, Acta Mater. **60** (2012) 4540-4550.
18. W.J. Lee, Y. Kim, E.D. Case, Journal of Materials Science. **28** (1993) 2079-2083.
19. G. Ziegler, J. Heinrich, Ceramurgia International. **6** (1980) 25-30.
20. L. Wang, J.L. Shi, J.H. Gao, D.S. Yan, Journal of the European Ceramic Society. **21** (2001) 1213-1217.
21. S. Maensiri, S.G. Roberts, Journal of the European Ceramic Society. **22** (2002) 2945-2956.
22. P.F. Becher, W.H. Warwick, in: Thermal Shock and Thermal Fatigue Behavior of Advanced Ceramics, NATO ASI Series. Munich, Germany, 1993, pp. 37-48.
23. F.P. Incropera, D.P. Dewitt, T.L. Bergman, A.S. Lavine, Fundamentals of Heat and Mass Transfer, sixth ed., John Wiley & Sons, Asia, 2007.
24. C.Y. Han, P. Griffith, The Mechanism of Heat Transfer in Nucleate Pool Boiling, MIT Technical Report No.19 for the Office of Naval Research, Massachusetts, 1962.
25. J.T. Cieslinski, K.A. Krygier, Experimental Thermal and Fluid Science. **59** (2014) 258-263.
26. J. Diao, D. Ren, J.R. Engstrom, K.H. Lee, Analytical Biochemistry. **343** (2005) 322-328.
27. B. Arkles, Hydrophobicity, Hydrophilicity, and Silanes. Reprinted from the October 2006 issue of Paint & Coatings Industry magazine, Morrisville, 2006.
28. F. Song, S. Meng, X. Xu, Y. Shao, Physical Review Letters. **104** (2010) 125502.
29. L.W. Fan, J.Q. Li, D.Y. Li, L. Zhang, Z.T. Yu, International Journal of Heat and Mass Transfer. **76** (2014) 81-89.
30. J. Liang, C. Wang, Y. Wang, L. Jing, X. Luan, Scripta Materialia. **61** (2009) 656-659.
31. Z. Zhou, F. Song, Y. Shao, S. Meng, C. Jiang, J. Li, Journal of the European Ceramic Society. **32** (2012) 3029-3034.
32. S. H. Yang, W.P. Baek, S.H. Chang, Int.comm. Heat Mass Transfer. **24** (1977) 1093-1102.
33. W. Peyayopanakul, J.W. Westwater, Int. J. Heat Mass Transfer. **21** (1978) 1437-1445.
34. R. Hu. (2011, April 13). Class Material of 22.313 Thermal-Hydraulics in Power Technology in Spring Semester 2011 at MIT Graduate School. *Laboratory Problem #4 Crud Effect on Cladding Temperature during LBLOCA, Combined Relap5 simulation and predictions by stand-alone models*. Cambridge, MA, U.S.A: MIT Department of Nuclear Science and Engineering.